Mansoura Engineering Journal, (MEJ), Vol. 36, No. 2, June 2011. M. 1

Nanofluid Convection Heat Transfer Behavior in a Heated Circular Tube

خصائص إنتقال الحراره فى انبوب دائرى يعمل بحبيبات النانو

Ali.M.Radwan(١), Ahmed.A.sultan(٢), L.H.Rabee(٣) and Ali Elbouz(٤).

(١) demonstrator of Mech.power engng. email : ali_radwan@mans.edu.eg

(٢) prof.of Mech.power engng. email : AAsultan@mans.edu.eg

(٣) prof.of mech.power engng.

(٤) lecture of Mech.power engng.

faculty of engineering , mansoura university.

ملخص البحث

فى هذا البحث تم عمل دراسه رقميه لخصائص انتقال الحراره بالحمل الجبرى الرقائقى خلال انبوب دائرى ذو فيض حرارى ثابت عند الجدار ويعمل بموائع النانو وذلك فى منطقه السريان كامل النمو. استخدم برنامج فلونت ٦.٣.٢٦ لعمل الحسابات .النتائج النظريه التى تم الحصول عليها كانت لكل من اكسيد الالمونيوم واكسيد النحاس بتركيزات مختلفه تتراوح بين ١ الى ٤ % نسبه حجميه . تم مقارنه نتائج انتقال الحراره والاحتكاك بمعادلات انتقال الحراره والاحتكاك المعروفه وذلك للتأكد من النتائج. اوضحت النتائج ان اضافه حبيبات النانو فى الماء النقى يعمل على زياده معامل انتقال الحراره بالحمل الجبرى والذى يزداد ايضا بوضوح مع زياده نسبه التركيز الحجميه وكذلك مع رقم رينولدز.

Abstract

In the present paper, the problem of forced convection laminar flow of nanofluids has been investigated for a uniformly heated circular tube. Numerical results, obtained by fluent ٦.٣.٢٦ code, for aluminum oxide nanoparticles (aluminium oxide) and copper oxide nanoparticles mixed with pure water with different volume fraction varied between ١% to ٤% by volume . The results were compared with that of pure water for the code validation and shows that the inclusion of nanoparticles in the base fluids has produced a considerable augmentation of the heat transfer coefficient that clearly increases with an increase of the particle concentration. The heat transfer enhancement also increases considerably with an augmentation of the flow Reynolds number. A comparison of heat transfer coefficient for each nanofluid was developed .

Accepted June 22, 2011.

1. Introduction

Heat transfer fluids such as water, mineral oil and ethylene glycol play a vital role in many industrial processes, including power generation, chemical processes, heating or cooling processes, and microelectronics. The poor heat transfer properties of these common fluids compared to most solids is a primary obstacle to the high compactness and effectiveness of heat exchangers. The essential initiative is to seek the solid particles having thermal conductivities several hundreds of times higher than those of conventional fluids. An innovative idea is to suspend ultrafine solid particles in the fluid for improving the thermal conductivity of a fluid. Many types of particle, such as metallic, non-metallic and polymeric, can be added into fluids to form slurries. However, the usual slurries, with suspended particles in the order of millimeters or even micrometers may cause some severe problems. Nanofluids are engineered by suspending nanoparticles with average sizes below 100 nm in traditional heat transfer fluids such as water, oil, and ethylene glycol. A very small amount of guest nanoparticles, when dispersed uniformly and suspended stably in host fluids, can provide dramatic improvements in the thermal properties of host fluids. Use of high thermal conductivity metallic nanoparticles (e.g., copper, aluminum, silver and silicon) increases the thermal conductivity of such mixtures, thus enhancing their overall energy transport capability [9].

Most solids, in particular metals, have thermal conductivities much higher compared to that of liquids. Hence, one can then expect that fluid containing solid particles may significantly increase its conductivity. Following the historical and pioneer work published hundred years ago. Pak and Cho [1] studied the hydrodynamic and heat transfer of dispersed fluids with submicron metallic oxide particles. Putra et al. [2] investigated the temperature dependence of thermal conductivity enhancement for nanofluids. A detailed investigation of increase of thermal conductivity with temperature was carried out . Wen and Ding [3], Heris, Esfahany, and Etemad [4] and S.M. Fotukian, M. Nasr Esfahany [5] are investigated experimentally the forced convection heat transfer of water–γAl_2O_3 nanofluids inside a circular tube with different boundary conditions. They reported that The enhancement was particularly significant in the entrance region, and was much higher than that solely due to enhancement on thermal conduction. Praveen K. Namburu and others [6], Samy Joseph Palm and others[7] are analyzed numerically the turbulent flow and heat transfer of AL_2O_3 in water mixture flowing through a circular tube under constant heat flux condition. They have clearly shown that the inclusion of nanoparticles into the base fluids has produced a considerable augmentation of the heat transfer coefficient that clearly increases with an increase of the particle concentration. H. Masuda, A. Ebata [8] have shown that by adding small solid particles in gas, the heat transfer coefficient can considerably be augmented. For liquid-solid particle mixtures, significant heat transfer enhancement was also observed as well as well Xuan, Y.M.; Li, Q.[9]. Such enhancement is due, in part, to the increase of the fluid effective thermal conductivity. On the other hand, it is believed that the reduction of the thermal boundary layer thickness due to the presence of particles and their random motion within the base fluid may have important contributions to such heat transfer improvement as well.

2. Thermo physical properties of nanofluids

Thermo physical properties of nanofluids are calculated by using the formulas summarized by Buongiorno [10]. The following relation can be used for calculating nanofluid density:-

$$\rho_{nf} = \varphi\rho_p + (1-\varphi)\rho_{bf} \quad (1)$$

It should be noted that for calculating the specific heat of nanofluid some of prior researchers have used the following correlation

$$c_{nf} = \varphi c_p + (1-\varphi)c_{pf} \quad (2)$$

It is modified in our analysis to Eq. (3) presented by Buongiorno [10] which is more accurate.

$$c_{nf} = \frac{\phi\rho_p c_p + (1-\phi)\rho_{bf}c_{bf}}{\rho_{nf}} \quad (3)$$

Batchelor [11] considered the effect of the Brownian motion of particles for an isotropic suspension of rigid and spherical particles, and the viscosity of nanofluid can be calculated there for by:-

$$\frac{\mu_{nf}}{\mu_{bf}} = (1 + 2.5\varphi + 6.5\varphi^2) \quad (4)$$

The most commonly used thermal conductivity equation (5) was proposed by Hamilton and Crosser [12] for the mixtures containing micrometer size particles. It is assumed that this equation is applicable for the nanofluids.

$$\frac{k_{nf}}{k_{bf}} = \frac{k_p + (n-1)k_{bf} - (n-1)\phi(k_{bf} - k_p)}{k_p + (n-1)k_{bf} + \phi(k_{bf} - k_p)} \quad (5)$$

In the above equation n is the shape factor and is equal to 3 for spherical nanoparticles. X. Zhang et al. [13] have shown that this correlation accurately predicts the thermal conductivity of nanofluids.The properties of base fluid (water) at different temperatures are available in ASHRAE [14].

3. Mathematical modeling

Fluent 6.3.26 code was used to simulate and solve our heat transfer problem. The first step of solving this problem is the geometrical configuration which is established by the fluent drawing tool known as GAMBIT®which used to create the model. Due to symmetry of the problem about tube axis , half of the tube is to be modeled neither using whole of the tube so as to reduce the computations .the first step of drawing the model is creating the end boundary points and connecting these boundaries to develop edges after that we make the face which connect the whole edges .This face will be meshed and then the mesh will be exported to Fluent 6.3.26 code after this the boundary conditions was entered into the code and the program will solve the governing equation at each node in the face until reaching an arbitrary error less than 10^{-6} .

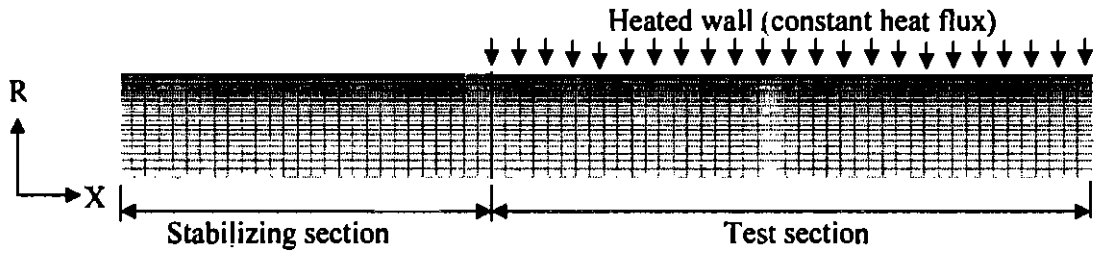

Fig. 1. Grid layout used in the present analysis, axisymmetric about X-axis.

3.1. Geometrical configurations and governing equations

Fig.1 shows the geometrical configurations under consideration. It consists of the steady, forced convection laminar flow and friction factor characteristics of a nanofluid flowing inside a straight tube of circular cross-section in two dimensions. The fluid enters with uniform temperature and axial velocity profiles at the inlet section. The tube is long enough so that the fully developed flow conditions prevail at the outlet section. The entrance length also is estimated for the design of the experimental test rig which will prepared for our experimental research of heat transfer in circular tube fitted with wire coil inserts and operating with nanofluids.

3.2. Assumptions

There exists no formulated theory to date that could reasonably predict the flow behaviors of a nanofluid by considering it as a multicomponent material. It should be noted that most nanofluids used in practical applications of heat transfer purposes are usually composed of particles finer than 40 nm. In such extremely reduced dimension, it has been suggested that these particles may be easily fluidized and consequently, can be considered to behave more like a fluid [15]. Furthermore, by assuming negligible motion slip between the particles and the continuous phase, and the thermal equilibrium conditions also prevail, the nanofluid may be then considered as a conventional single-phase fluid with effective physical properties being function of the properties of both constituents and their respective concentrations [1]. An interesting result from such an assumption resides in the fact that an extension from a conventional fluid to a nanofluid appears feasible, and one may expect that the classic theory as developed for conventional single- phase fluids can be then applied to nanofluids as well. Thus, all the equations of conservation (mass, momentum and energy) as well known for single-phase fluids can be directly extended and employed for nanofluids.

In the present work, we have adopted the single phase fluid approach in order to be able to study the thermal behaviors of nanofluids. For the particular applications under consideration, we have assumed that the nanofluids are incompressible with constant physical properties. Also, both the compression work and viscous dissipation are assumed negligible in the energy equation. Under such conditions, the general conservation equations written in the vector form are as follows (Warsi, [16]; Eckert and Drake[17]).

- Conservation of mass :-

$$div(\rho V) = 0 \quad (6)$$

- Conservation of momentum :-

$$div\ (\rho VV) = -grad\ P + \mu\nabla^2 V \quad (7)$$

- Conservation of energy :-

$$div(\rho V C_p T) = div(K\ grad(T)) \quad (8)$$

In the above equations, V, P and T are respectively fluid velocity vector, pressure and temperature. All fluid properties are evaluat d at the reference temperature that is the fluid inlet temperature T_0 = 300 K.

3.3. Boundary conditions:

As shown above in Fig.1 only half of the tube was modeled due to the symmetry for reduction of numerical calculations. The governing equations from (6) to (8) constitute a highly non-linear and coupled equation system that must be solved under the appropriate boundary conditions. For our problem stabilizing section was designed to reach fully developed flow in the circular tube and simultaneously thermally developing region. It is assumed that at the tube inlet, a uniform axial velocity V_0, temperature T_0 prevail. Outflow boundary condition has been implemented for the outlet section. This boundary condition implies zero normal gradients for all flow variables except pressure. On the tube wall, the usual non-slip conditions are imposed; also the uniform wall heat flux is assumed at the tube wall of about 8000 W/m^2 . The variation of velocity value at the inlet will be assumed to achieve laminar flow regime in our study according to the tube diameter. At the lower wall of the modeled domain, the axis boundary condition was applied. Boundary conditions of the problem can be summarized as shown in Fig.2.

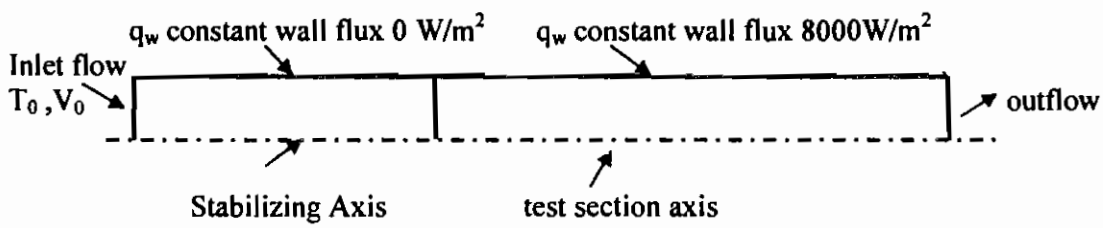

Fig.2 Model applied boundary conditions

4. Numerical method

The steps of solution of this problem using Fluent6.3.26 code can be achieved by establishing the geometry and the gird by using GAMBIT®, the preprocessing module of the FLUENT code. The mesh then exported to fluent 6.3.26.The computational fluid dynamics Fluent 6.3.26 was used for solving this problem. The systems of governing equations from (6) to (8) were solved by control volume approach. Control-volume technique converts the governing equations to a set of algebraic equations that can be solved numerically. The control volume approach employs the conservation statement or physical law represented by the entire governing equations over finite control volumes. Grid schemes used are staggered in which velocity components are evaluated at the center of control volume interfaces and all scalar quantities are evaluated in the center of control volume. Fluent 6.3.26 solves the linear systems resulting from discretization schemes using a point implicit (Gauss–Seidel) linear equation solver in conjunction with an algebraic multigrid method. During the iterative process, the residuals were carefully monitored. For all simulations performed in the present study, converged solutions were considered when the residuals resulting from iterative process for all governing equations were lower than 10^{-6}.

4.1. Grid optimization

The grid used in the present analysis was 30 × 1650, 30 in r-direction and 1650 in x-direction. We also tested 40×2000 and 50×2500. All gave similar values of velocity and temperature at the outlet. Therefore, 30×1650 was accepted as the optimal grid size. This grid size was validated by our CFD results in Figs. 3 and 4.

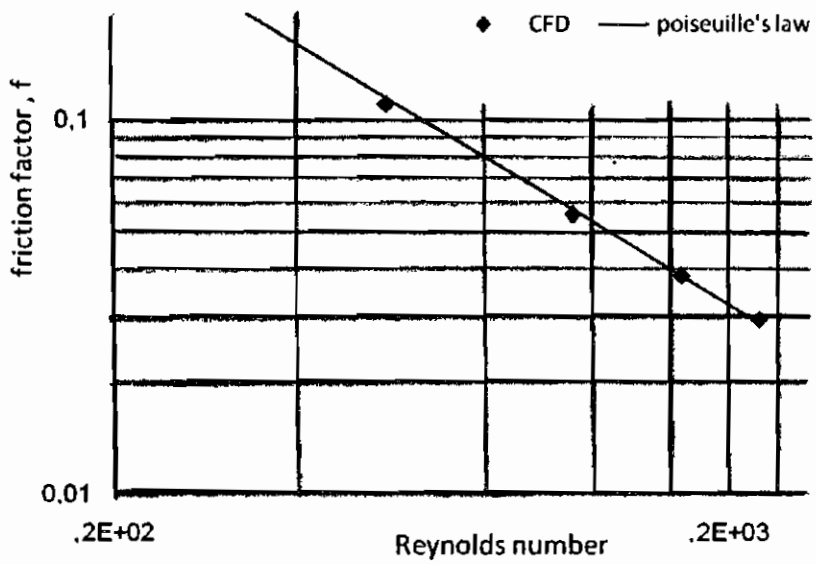

Fig. 3. Comparison of Darcy friction factor by Poiseuilles formula and computed values for pure water in laminar regime

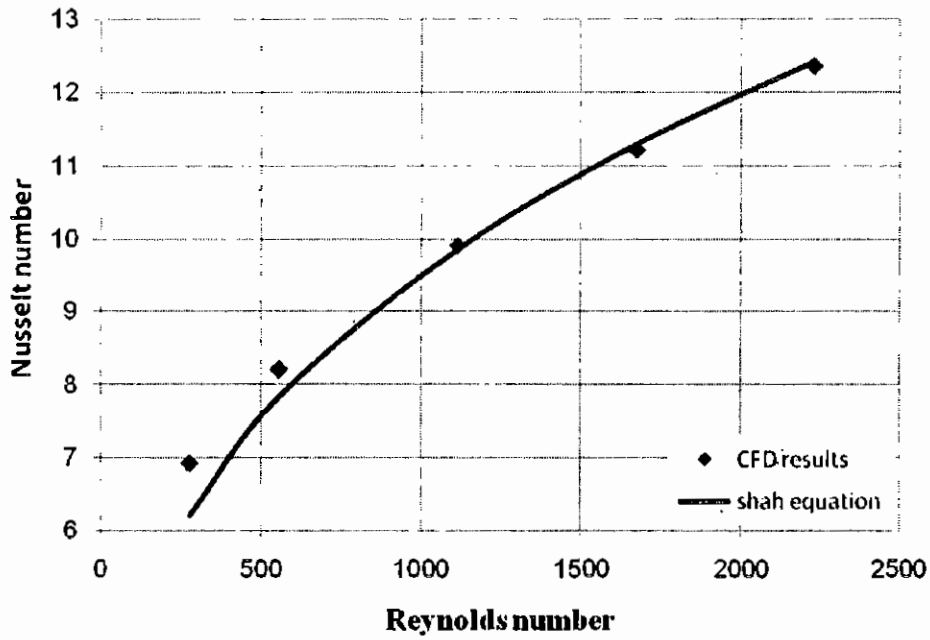

Fig. 4. Comparison of average Nusselt number by Shah equation and computed values for pure water in laminar regime.

4.2. Validation of the present simulation

By applying the previous boundary conditions and allowing for the fluent code to solve the problem we first checking for hydro-dynamically fully develop region and to identify the hydrodynamic entrance length and next applying the thermal boundary condition after that entrance length. The tube has a diameter of 14 mm and a length of 1650 mm. The fluid enters the tube with a constant inlet temperature T_0 of 27°C and with uniform axial velocity V_0. The Reynolds number was varied from 278 to 2229. In order to validate the computational model, the numerical results were compared with the theoretical data available for the conventional fluids. The Darcy friction factor given by Poiseuille's is presented using Eq. (9) from Frank White [18].

$$f = 64/Re \quad (9)$$

Figure 3 displays the comparison of Darcy friction factor from Poiseuilles formula and computed values from the present simulations. An excellent agreement is observed with maximum deviation and average deviation of computed values from theoretical equation being 4.11% and 2.14 %, respectively, over the range of Reynolds numbers studied. Next, the Nusselt number for the fully developed laminar flow regime and constant heat flux boundary conditions was compared by existing correlations, Shah [19] was developed the correlation of heat transfer in laminar flows under the constant heat flux boundary conditions which are given by equation 10 and 11.

$$Nu(x) = 1.935 \times (Re \times Pr \times \frac{D}{L})^{\frac{1}{3}} \quad \text{vallied for } \left(Re \times Pr \times \frac{D}{L}\right) \geq 33.3 \qquad (10)$$

$$Nu(x) = \left(4.364 + 0.0722 \times Re \times Pr \times \frac{D}{L}\right) \text{ vallied for } \left(Re \times Pr \times \frac{D}{L}\right) < 33.3 \qquad (11)$$

Where :-

$$Re = \frac{4m^{o}}{\pi D_i \mu_{nf}} \qquad (12) \qquad and \qquad Pr = \frac{C_{p-nf}\mu_{nf}}{k_{nf}} \qquad (13)$$

For steady and incompressible flow of nanofluids in a tube of uniform cross-sectional area, the Reynolds number and Prandtl number are defined as equation 12 and 13 respectively. Where m^0 is the mass flow rate and μ_{nf} , c_{p-nf} and k_{nf} are the viscosity, specific heat and thermal conductivity of nanofluids, respectively calculated by the equations from 1 to 5 .

Figure 4 displays comparison of Nusselt numbers obtained from the present numerical analysis in fully developed region for pure water with the equation given by Shah [19]. The maximum and average deviations of computed Nusselt number from the equation given by Shah is 11.4 % - at lower Reynolds number - and 3.6 %, respectively.

4.3. Checking for hydro-dynamically fully developed regime

As shown in Fig.1 the mesh was generated so as to reach fully developed hydro dynamic flow and enters the test section with this boundary condition and of non uniform velocity and the flow will begin in thermally developing of the boundary layer till it reach the thermally fully developed. Because the hydrodynamic entrance length is depending on the flow Reynolds number [18] and it increases with Reynolds number for laminar flow regime then validation of this relationship must be firstly done. Figure 5 shows the relation between axial flow velocity and axial distance along the tube. It is seen from the figure that the axial velocity increase with axial distance and reaches a maximum value at a certain distance and then remain constant. A maximum entry length of 0.8 m is reached at a Reynolds number of 2229 as shown from Fig.5. At this length the test section will be designed and a good agreement of the entrance length with that of calculated value which $L/D \geq 50$ [18] is found. Figure 6 show the variation of velocity profile along the cross section of the tube, at the same Reynolds number 2229 which give no change in the velocity profile after 0.8 m from the inlet of the tube so the hydro-dynamic entrance length will be 0.8 m for this tube diameter in case of laminar flow of water which agrees with the finding of reference [18].

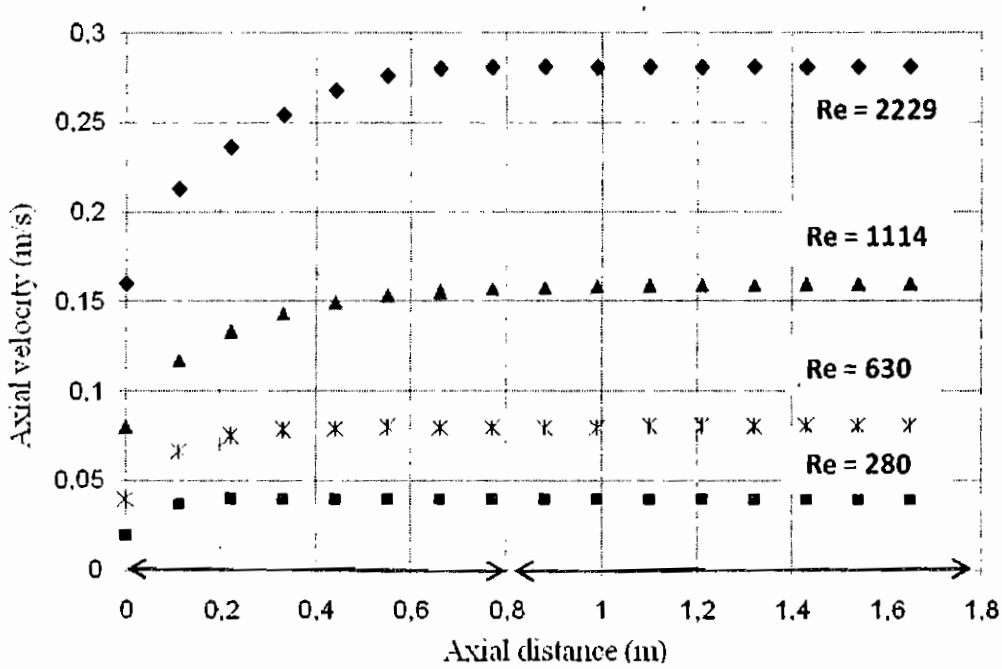

Fig.5 Axial centerline velocity variation along the tube length.

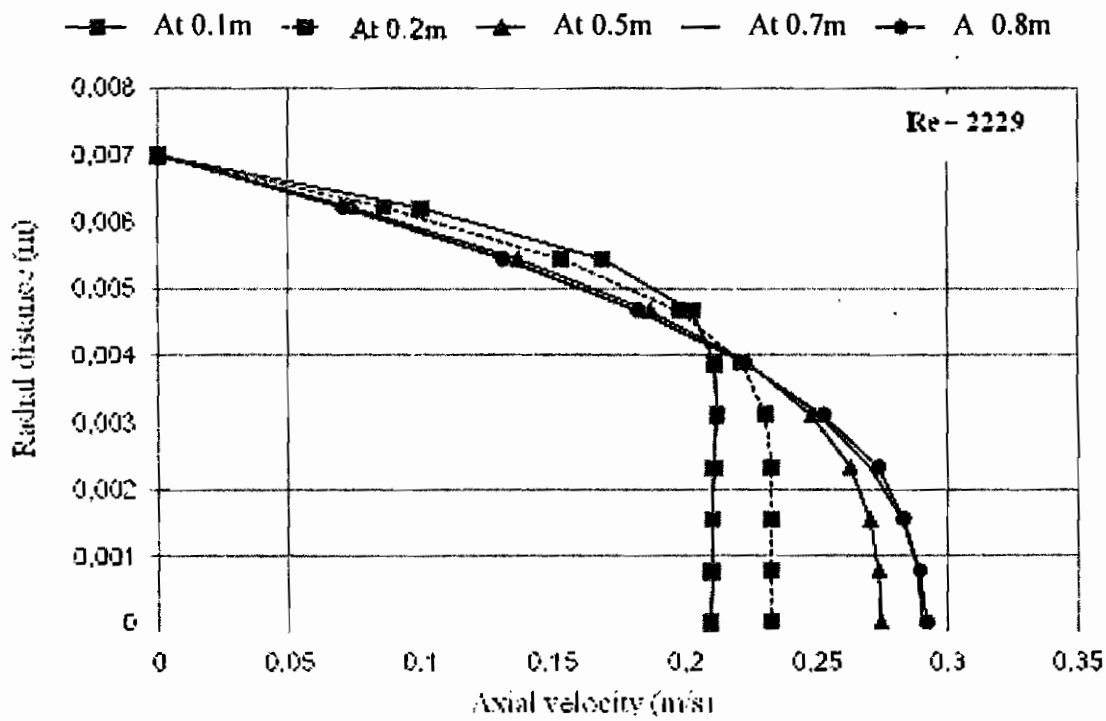

Fig.6 velocity profile variation at different distances from flow inlet.

5. Results of nanofluid

After validation of the results we can treat nanofluid as a single phase flow like water with different thermal properties [1].

5.1. Heat transfer results

We will discuss the effect of nanofluid volume fraction φ % of nano-particles dispersed in base fluid (water) on heat transfer coefficient and Nusselt number for both aluminum oxide and copper oxide nanoparticles with different concentrations over the range from 1 to 4% by volume. A comparison between the results of both nanoparticles results will be done.

5.1.1. Effect of nanoparticles volume fraction

Figure 7 displays the influence of Al_2O_3 nanoparticles volume concentration on the heat transfer coefficient .The computational results show that the heat transfer coefficient of nanofluid increase with Reynolds number and with particle concentration. As an example, the increase in the heat transfer coefficient is about 1.13 times with 4% volume concentration of Al_2O_3 nanoparticles over the base fluid (water) at Reynolds number of 320 and the increase in the heat transfer coefficient is about 1.117 times at Reynolds number of 2500. The increase in the heat transfer coefficient may be due to the increase in thermal conductivity of the nanofluid.

Figure 8 shows the Nusselt number variation of nanofluid with Reynolds number over the studied range. The results show that Nusselt number will increase with Reynolds number but decreases with the increase in the nanoparticles concentration. It may be due to the increase in nanofluid thermal conductivity that is much greater than the increase in the product of nanofluid density and specific heat.

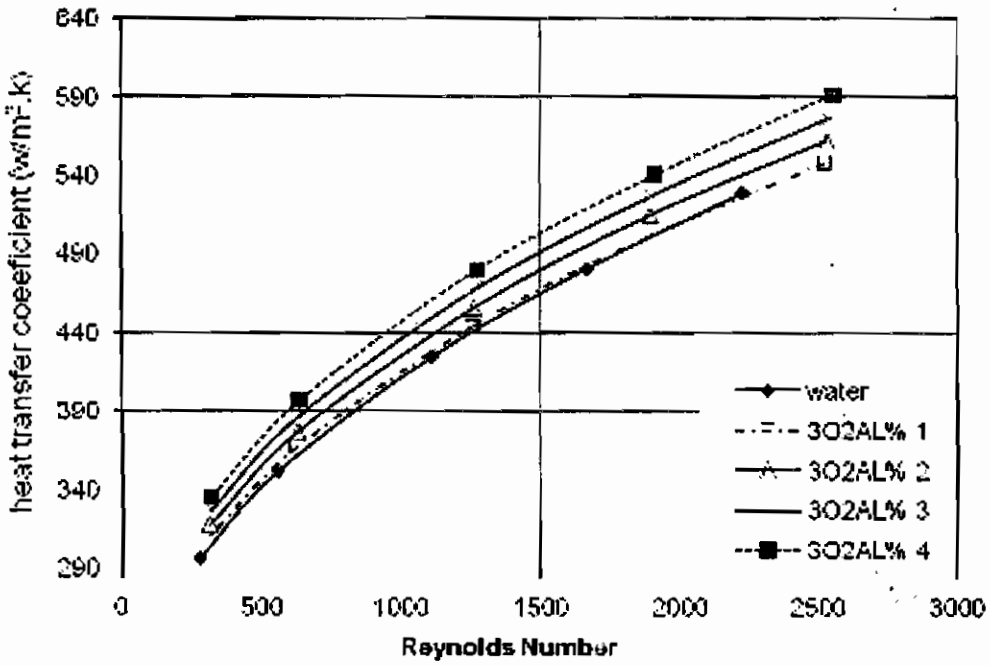

Fig. 7. The influence of AL_2O_3 nanoparticles volume concentration on the heat transfer coefficient.

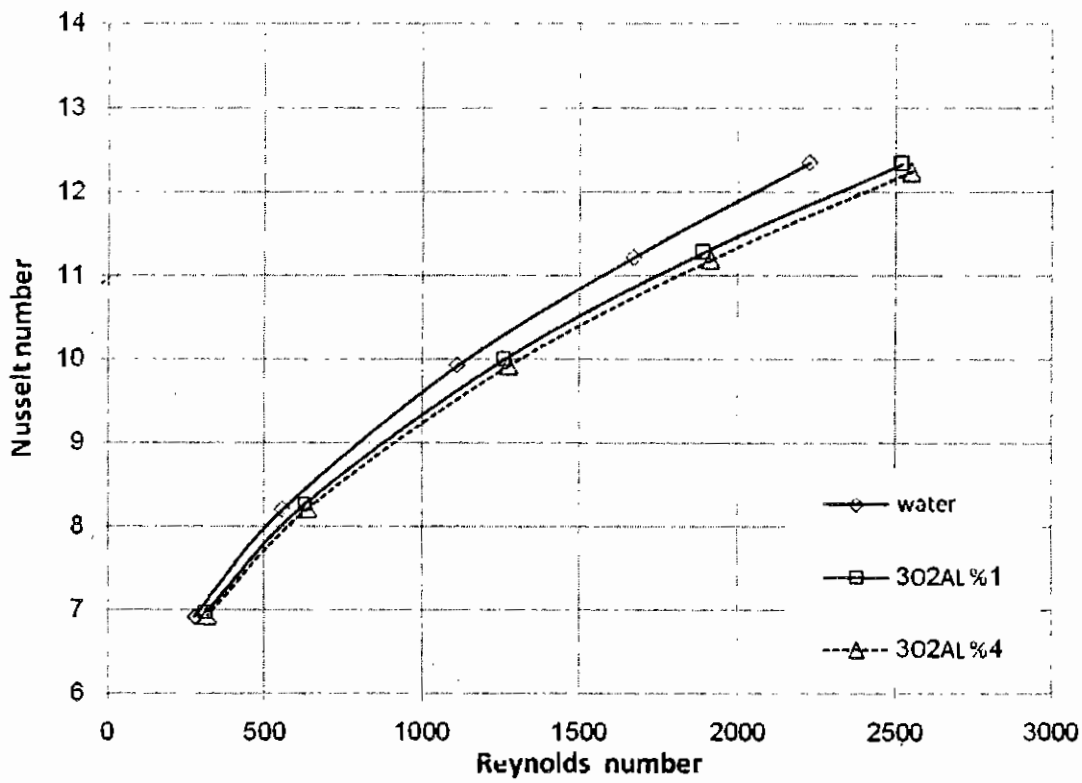

Fig.8 Nusselt number variation of AL_2O_3 nanofluid with Reynolds number

Figure 9 shows the influence of copper oxide nanoparticles volume concentration on the heat transfer coefficient over a range of Reynolds numbers. The computational fluid dynamic (CFD) results show an increase in heat transfer coefficient with Reynolds number and the volume concentration of nanoparticles. For example the heat transfer coefficient increases by about 1.15 times that for pure water at Reynolds number of 320 with 4% volume concentration of copper oxide and increases of about 1.12 times at a Reynolds number of 2500.

Figure 10 shows the Nusselt number variation of copper oxide nanofluid with Reynolds number. The results indicate also that Nusselt number increases with Reynolds number and decreases with the increase in percentage volume. This is due to the same reason mentioned in the previous discussion.

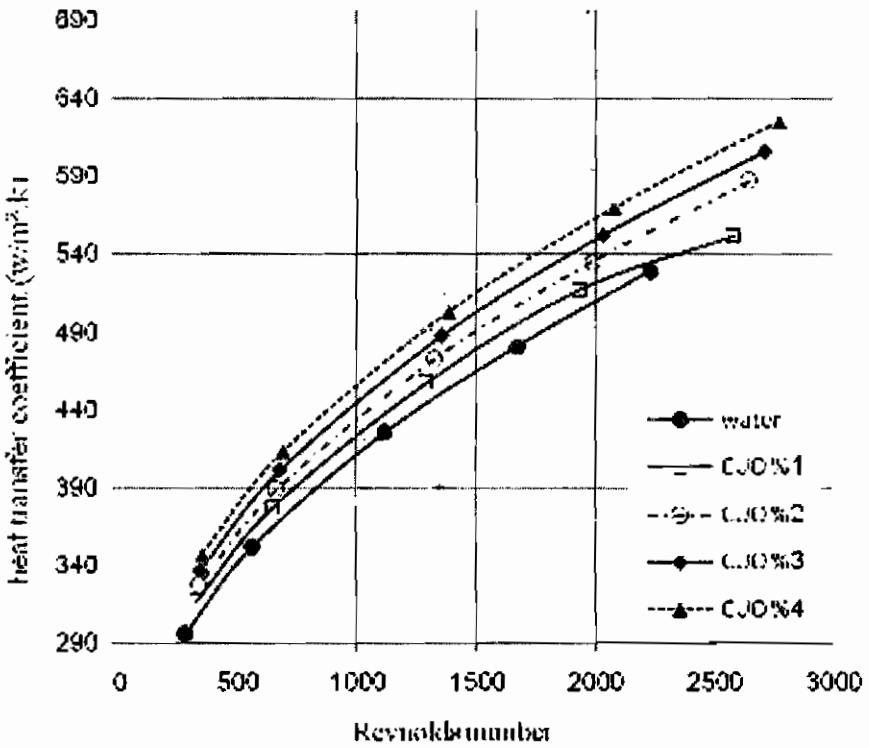

Fig. 9. The influence of CUO nanoparticles volume concentration on the heat transfer coefficient over a range of Reynolds numbers.

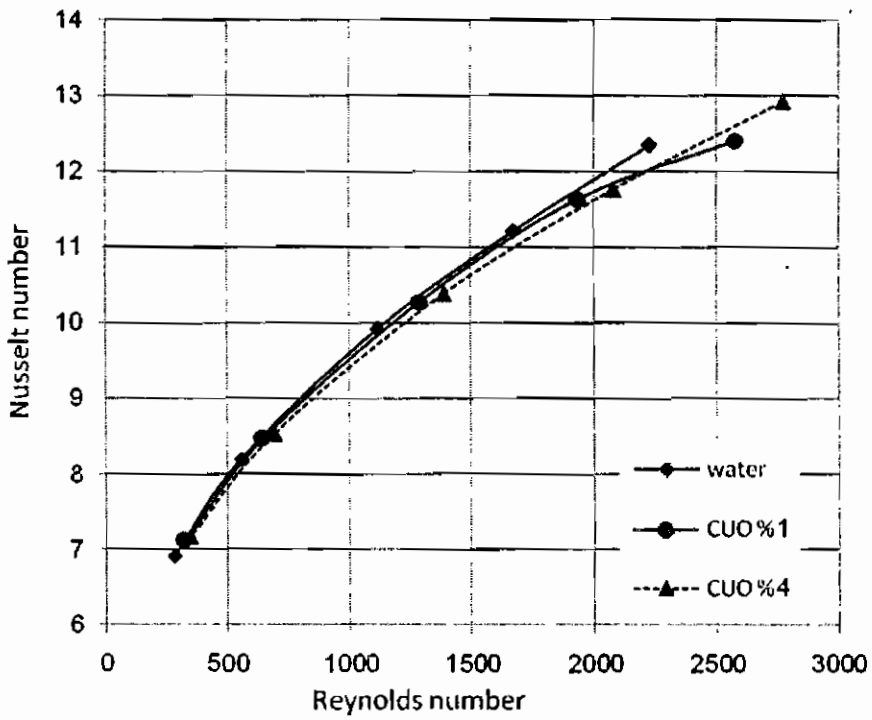

Fig.10 Nusselt number variation of CUO nanofluid with Reynolds number

Figure 11 presents a comparison of heat transfer coefficients of nanofluid of copper oxide and aluminum oxide nanoparticles and the enhancement of heat transfer coefficient as well. The results show that the copper oxide nanofluid is more efficient in heat transfer than aluminum oxide .This may be due to the thermal conductivity of copper oxide is higher than that for aluminum oxide nanofluid. Figure 12 and 13 show the variation of heat transfer coefficient with volume concentration at different Reynolds numbers of copper oxide and aluminum oxide respectively. It can be seen that the heat transfer coefficient increases with volume concentration and Reynolds number.

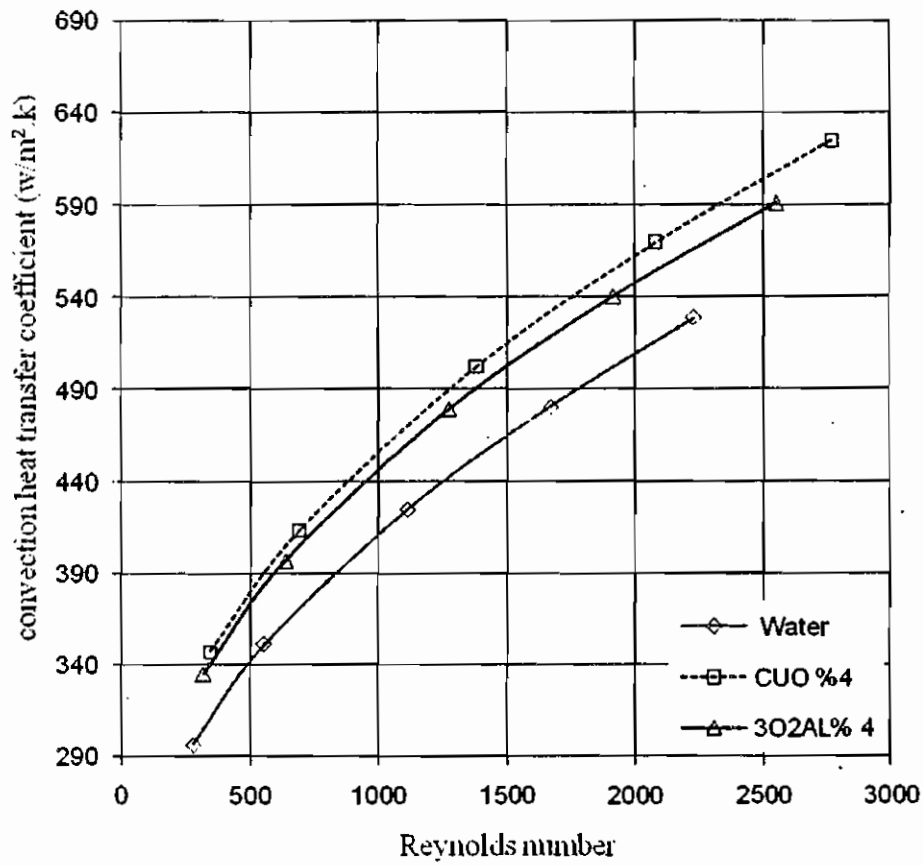

Fig.11 comparison between aluminum oxide and copper oxide nanofluid

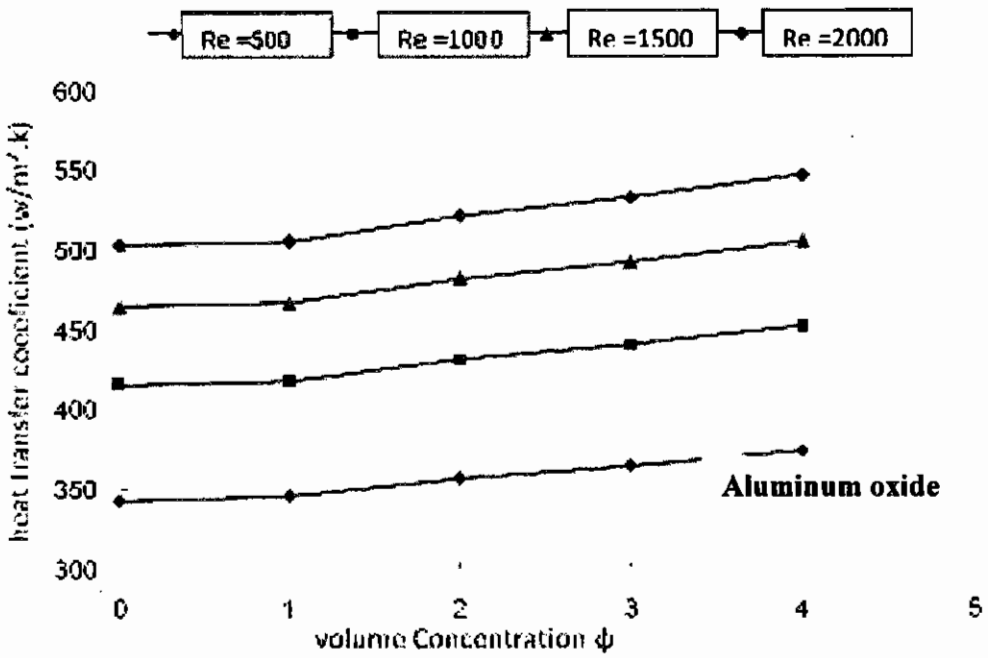

Fig.12 heat transfer coefficient variation with volume concentration at different Reynolds numbers of AL_2O_3 nanofluid

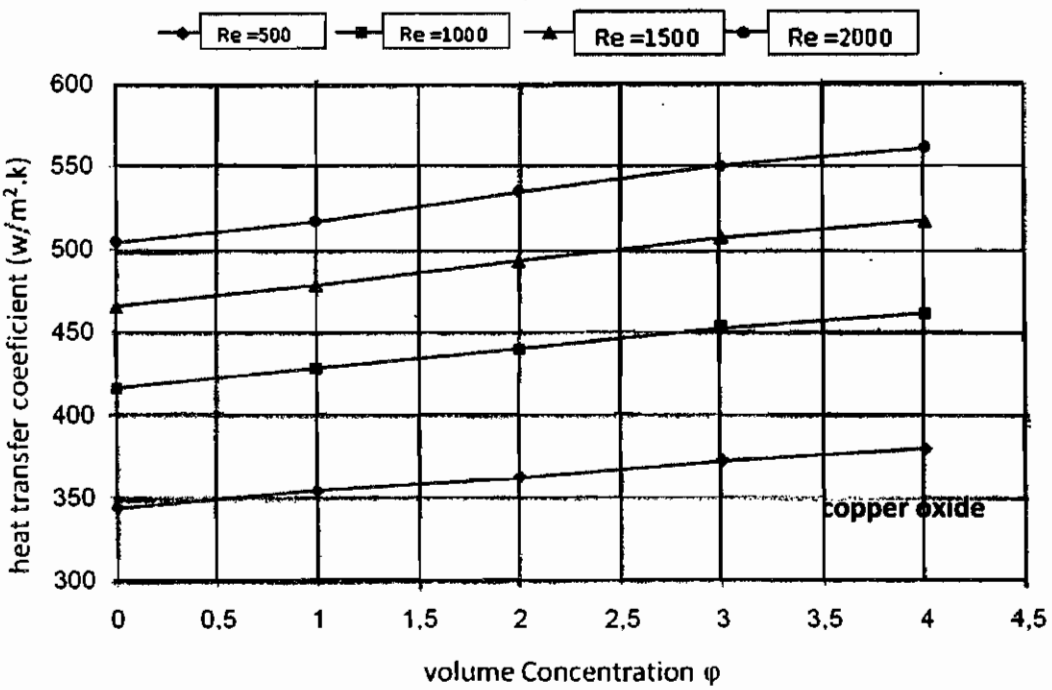

Fig.13 heat transfer coefficient variation with volume concentration at different Reynolds numbers of copper oxide nanofluid

5.2. Friction coefficient results

Figure14 shows the relation between friction coefficient of nanofluid and Reynolds number for two nanoparticle materials, namely AL_2O_3 and CUO and nanoparticles concentration of 1% and4%. It is shown from the figure that the friction coefficient strongly depends on Reynolds number and is weakly affected by both nanoparticle materials and concentration. The figure shows that the friction coefficient decreases with the increase in Reynolds number and remains nearly constant with nanoparticle materials and volumetric concentration.

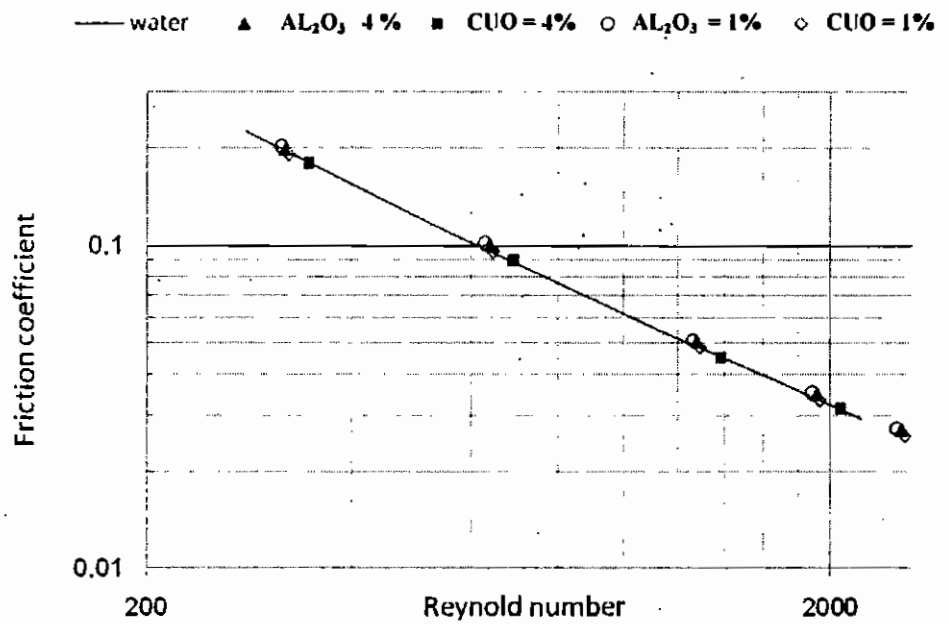

Fig.14 friction coefficient variation with the Reynold number

6. Conclusions

From the above numerical results of the heat transfer and friction factor of nanofluids of different nanoparticles concentration and materials for laminar flow through circular tube in hydraulic fully developed region. The following conclusions can be made:-

1- The heat transfer coefficient increase with Reynolds number and nanoparticle concentration.
2- The heat transfer coefficients strongly affected by nanofluids effective thermal conductivity which depends on both nanoparticles and fluid thermal conductivity.
3- The Nusselt number decreases with both nanoparticle concentration and thermal conductivity due to the effect of thermal conductivity on Nusselt number over that the effect of heat capacity (ρc_p).
4- The friction coefficient increases with Reynolds number and remains nearly unaffected by nanoparticle concentration and material type.

References

[1] Pak, B.C., and Cho, Y.I., 1998. Hydrodynamic and heat transfer study of Dispersed fluids with submicron metallic oxide particles. Experiment. Heat Transfer 11 (2), 151–170.

[2] Putra Nandy, Thiesen Peter and Roetzel Wilfried., 2003, "Temperature dependence of thermal conductivity of nanofluids" Journal of Heat Transfer 125. 567-574.

[3] Wen Dongsheng, and Ding Yulong.,2004,"Experimental investigation into convective heat transfer of nanofluids at the entrance region under laminar flow conditions" International Journal of Heat and Mass Transfer, 47. 5181-5188.

[4] Heris, S. Z., Esfahany, M. N., Etemad, S. G. 2007. Experimental Investigation of Convective Heat Transfer of Al_2O_3/water Nanofluid in Circular Tube. International Journal of Heat and Fluid Flow, 28(2007).203-210.

[5] S.M. Fotukian, M. Nasr Esfahany.2010." experimental study of turbulent convective heat transfer and pressure drop of dilute CuO/water nanofluid inside a circular tube". International communications in Heat and Mass Transfer. 37 (2010) 214–219.

[6] Praveen K. Namburu, Debendra K. Das, Krishna M. Tanguturi, Ravikanth S. Vajjha,2008." Numerical study of turbulent flow and heat transfer characteristics of nanofluids considering variable properties". International Journal of Thermal Sciences. 1-13.

[7] Samy Joseph Palm and et-al, 2005 ," Heat transfer enhancement by using nanofluids in forced convection flows". International Journal of Heat and Fluid Flow 26 (2005) 530–546.

[8] H. Masuda, A. Ebata, K. Teramae, N. Hishinuma, Alteration of thermal conductivity and viscosity of liquid by dispersing ultra-fine particles (dispersion of Al2O3, SiO2, and TiO2 ultra-fine particles), Netsu Bussei 4(1993) 227.

[9] Xuan, Y.M.; Li, Q. ,2003,"Investigation on convective heat transfer and flow features of nanofluids". Journal of heat transfer, 125, 151-155.

[10] J. Buongiorno, Convective transport in nanofluids, Journal of Heat Transfer 128 (2006) 240–250.

[11] G.K. Batchelor, The effect of Brownian motion on the bulk stress in a suspension of spherical particles, J. Fluid Mech. 83 (1) (1977) 97–117.

[12] R.L. Hamilton, O.K. Crosser, Thermal conductivity of heterogeneous two component systems, Indus. Eng. Chem. Fundam. 1 (3) (1962) 187–191.

[13] X. Zhang, H. Gu,M. Fujii, Effective thermal conductivity and thermal

diffusivity of nanofluids containing spherical and cylindrical nanoparticles, Journal of Applied Physics 100 (4) (2006) 044325, 1–5.

[14] ASHRAE Handbook Fundamentals, American Society of Heating, Refrigerating and Air-Conditioning Engineers Inc., Atlanta, 2005.

[15] Xuan, Y.M.; Li, Q., 2003,"Investigation on convective heat transfer and flow features of nanofluids". Journal of heat transfer, 125, 151-155

[16] Warsi, Z.U.A., 1999. Fluid Dynamics Theoretical and Computational approaches, second ed. CRC Press, Boca Raton, Florida, USA.

[17]Eckert, E.R.G., Drake Jr., R.M., 1972. Analysis of Heat and Mass Transfer. McGraw-Hill, New York, USA.

[18] F.M. White, Viscous Fluid Flow, McGraw Hill, New York, 1991.

[19] R.K. Shah, M.S. Bhatti, Laminar convective heat transfer in ducts, in: S. Kakac R.K. Shah, W. Aung (Eds.), Handbook of Single-Phase Convective Heat Transfer, Wiley, New York, 1987 (Chapter 3).